

# Soft Matter

Accepted Manuscript



This article can be cited before page numbers have been issued, to do this please use: V. Sharma, S. K. Ghosh, P. Mandal, T. Yamada, K. Shibata, S. Mitra and R. Mukhopadhyay, *Soft Matter*, 2017, DOI: 10.1039/C7SM01799E.



This is an Accepted Manuscript, which has been through the Royal Society of Chemistry peer review process and has been accepted for publication.

Accepted Manuscripts are published online shortly after acceptance, before technical editing, formatting and proof reading. Using this free service, authors can make their results available to the community, in citable form, before we publish the edited article. We will replace this Accepted Manuscript with the edited and formatted Advance Article as soon as it is available.

You can find more information about Accepted Manuscripts in the [author guidelines](#).

Please note that technical editing may introduce minor changes to the text and/or graphics, which may alter content. The journal's standard [Terms & Conditions](#) and the ethical guidelines, outlined in our [author and reviewer resource centre](#), still apply. In no event shall the Royal Society of Chemistry be held responsible for any errors or omissions in this Accepted Manuscript or any consequences arising from the use of any information it contains.

# Effects of Ionic Liquids on the Nanoscopic Dynamics and Phase Behaviour of a Phosphatidylcholine Membrane

V. K. Sharma<sup>1</sup>, S. K. Ghosh<sup>2</sup>, P. Mandal<sup>2</sup>, T. Yamada<sup>3</sup>, K. Shibata<sup>4</sup>, S. Mitra<sup>1#</sup> and R. Mukhopadhyay<sup>1#\*</sup>

<sup>1</sup>Solid State Physics Division, Bhabha Atomic Research Centre, Mumbai 400085, India

<sup>#</sup>Homi Bhabha National Institute, Anushaktinagar, Mumbai 400094, India

<sup>2</sup>Department of Physics, Shiv Nadar University, Tehsil Dadri, G.B. Nagar 201314, India

<sup>3</sup>Neutron R&D Division, CROSS, Tokai, Ibaraki 319-1106, Japan

<sup>4</sup>Materials and Life Science Division, J-PARC Center, JAEA, Tokai, Ibaraki 319-1195, Japan

## Abstract

Ionic liquids (ILs) are potential candidates for new antimicrobials due to their tunable antibacterial and antifungal properties that are required to keep pace with the growing challenge of bacterial resistance. To a great extent their antimicrobial actions are related to the interactions of ILs with cell membrane. Here, we report effects of ILs on the nanoscopic dynamics and phase behaviour of the membrane of dimyristoylphosphatidylcholine (DMPC), a model cell membrane, as studied using neutron scattering techniques. Two prototypical imidazolium-based ILs 1-butyl-3-methylimidazolium tetrafluoroborate (BMIM[BF<sub>4</sub>]) and 1-decyl-3-methylimidazolium tetrafluoroborate (DMIM [BF<sub>4</sub>]) which differs only in terms of the alkyl chain length of cation, have been used for the present study. Fixed Elastic Window Scan (FEWS) shows that incorporation of ILs affects the phase behaviour of the phospholipid membrane significantly and the transition from solid gel to fluid phase shifts to lower temperature. This is found to be consistent with our differential scanning calorimetry measurements. DMIM[BF<sub>4</sub>] which has longer alkyl chain cation, affects phase behaviour more strongly in comparison to BMIM[BF<sub>4</sub>]. The pressure-area isotherms of DMPC monolayer measured at air-water interface show that in the presence of ILs, isotherms shift towards the higher area-per lipid molecules. DMIM[BF<sub>4</sub>] is found to shift isotherm in greater extent compared to BMIM[BF<sub>4</sub>]. Quasielastic neutron scattering (QENS) data shows that both ILs act as a plasticizer, which enhances the fluidity of the membrane. DMIM[BF<sub>4</sub>] is found to be a stronger plasticizing agent in comparison to BMIM[BF<sub>4</sub>] that has cation of shorter alkyl chain. Incorporation of DMIM[BF<sub>4</sub>] enhances not only the long range lateral motion but also the localised internal motion of the lipids. On the other hand, BMIM[BF<sub>4</sub>] acts weakly in comparison to DMIM[BF<sub>4</sub>] and mainly alters the localised internal motion of the lipids. Any subtle change in the dynamical properties of the membrane can profoundly affect the stability of the cell. Hence, the dominant effect of the IL with longer chain length on the dynamics of the phospholipid membrane might be correlated with their cytotoxic activity. QENS data analysis has provided a quantitative description of the effects of two imidazolium-based ILs, on the dynamical and phase behaviour of the model cell membrane, which is essential for detailed understanding towards their action mechanism.

**Keywords:** Ionic liquids, Phospholipid membrane, Dynamics, QENS, Elastic intensity scan,

\*Corresponding Author: Email: [mukhop@barc.gov.in](mailto:mukhop@barc.gov.in), FAX: +91-22-25505151; Tel: +91-22-25594667

## Introduction

Ionic liquids (ILs) are the salt in which the ions are poorly coordinated, which results in their melting point below to 100°C [1]. Among them, some ILs are liquids even at room temperature and are known as room temperature ionic liquids (RTILs). In these salts, at least one ion has delocalized charge and one component is organic, which prevents the formation of a stable crystal lattice. ILs are designed with large organic cations, such as imidazolium or pyridinium, with alkyl chain substituent that alters the hydrophobicity of the molecule. Common IL anions include hexafluorophosphate ( $\text{PF}_6^-$ ), tetrafluoroborate ( $\text{BF}_4^-$ ), nitrate ( $\text{NO}_3^-$ ) and halide ( $\text{X}^-$ ) and so forth. ILs are generally known as ‘designer solvents’ and large combinations of potentially useful ILs have been made by variations in anions and cations [1, 2]. They are non-explosive, non-flammable, have good thermal stability and high ionic conductivity, hence can be used in various industrial applications such as chemical and polymer synthesis, energy harvesting, food and cellulose processing, waste recycling, and so on [1,3-4]. These ILs exhibit very low vapour pressure [5] but unlike other popular solvents (e.g., water, chloroform or methanol) they rarely evaporate. Hence, ILs are often considered to be environment-friendly ‘Green Solvents’ and do not contribute in air pollution [6]. However, release of ILs into aquatic environments may lead to water pollution. These molecules are amphiphilic in nature, hence can be dissolved in inorganic as well as organic solvents. Based on number of recent studies [2,7-8] their toxicity to living organisms has become an emerging issue. Although, the fundamental mechanisms, behind the IL toxicity, in most of the cases are not well understood, it has been suggested that one of the main reasons for this high level of toxicity is the molecular interactions between ILs and cell membranes [9-16]. For several antibiotics and antimicrobial peptides cell membrane is a prime target, as slight modification in the structure, dynamics or elastic properties can profoundly affect the stability of the cell and eventually leads to their death. It has been shown that ILs are antibacterial in nature since they inhibit the growth of many bacteria such as *E. coli*, *Bacillus subtilis*, and so forth [10,17]. Recent studies [18] showed that ILs are the potential candidates for new antimicrobials due to their antibacterial and antifungal properties. Furthermore, their physical and chemical properties and biological activities can be ‘finely tuned’ by the variations of the anion and cation. This unique, versatile property can help in designing of new antimicrobials that are required to keep pace with the rising challenge of antibiotic resistance. Cell membranes are a self assembled heterogeneous mixture of lipids, membrane integral proteins, and other small molecules such as carbohydrates [19]. Phospholipids are the main fundamental component of the cell membrane and the self assembled structure of these

molecules can be used as first order model of cell membrane. Phosphatidylcholine are the prime structural phospholipids of eukaryotic membranes [20]. In the present case, a saturated phosphatidylcholine, 1,2-dimyristoyl-sn-glycero-3-phosphocholine (DMPC) has been used to form the model biological membrane to study the interaction with ILs. Chemical structure of DMPC has been shown in Fig.1. Imidazolium-based cations are one of the popular classes of ILs and have been shown to be antimicrobial toward several classes of organisms [8,17-18]. It has been shown that the cytotoxicity strongly increases with the chain length of the IL cations [17]. Hence, it would be pertinent to investigate dependence of the alkyl chain length of IL cations towards the interaction with the membrane. Hence, two different imidazolium based ILs, 1-butyl-3-methylimidazolium tetrafluoroborate (BMIM[BF<sub>4</sub>]) and 1-decyl-3-methylimidazolium tetrafluoroborate (DMIM [BF<sub>4</sub>]) which differs only in terms of the alkyl chain length (C<sub>n</sub>H<sub>2n+1</sub>) of cations have been used in the present study. BMIM cation (C<sub>4</sub>mim) has an alkyl chain length of 4 carbon atoms whereas DMIM cation (C<sub>10</sub>mim) has an alkyl chain length of 10 carbon atoms. Schematic of a lipid bilayer and chemical structures of DMPC lipid, BMIM and DMIM cations are shown in Fig.1.

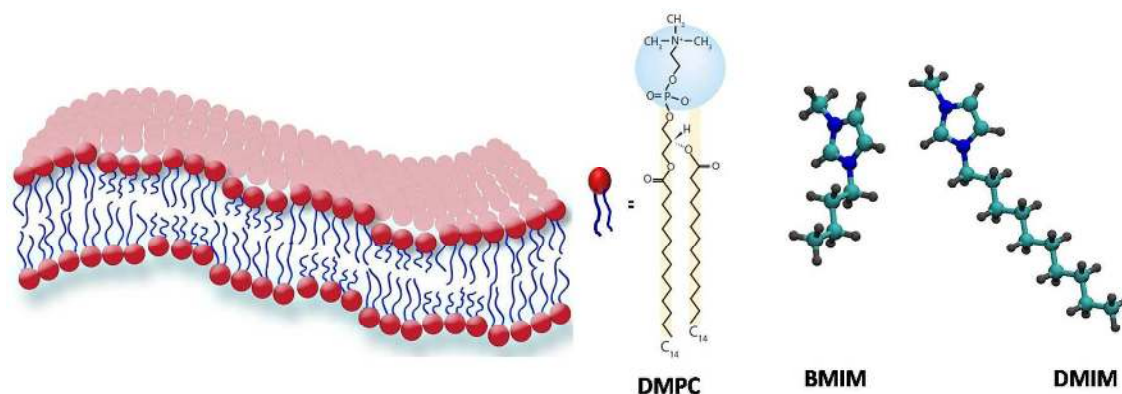


**Fig. 1** Schematic of lipid bilayer and chemical structures of lipid DMPC and cations of ionic liquids BMIM[BF<sub>4</sub>] and DMIM[BF<sub>4</sub>]. Both IL cations have same imidazolium head group but having different alkyl chain lengths.

In the last few years [9-16], different experimental and computational methods have been employed to understand the interaction between ILs and phospholipid membranes. Scanning electron microscopy (SEM), differential scanning calorimetry (DSC) and particle size analyzer have been used to investigate interactions of ionic liquids and cell membrane [9]. It has been shown that ILs are incorporated into cell membranes based on their

hydrophobic alkyl chains, resulting in perturbation of lipid membrane structure. It was found that penetration of ILs into lipid bilayer, and the efficiency of ILs increases as a function of both alkyl chain length and their concentration. Recently, X-ray and neutron reflectivity [10,11] measurements have been carried out to investigate the effects of IL on the structure of the bilayer membrane. It was found that due to penetration of IL into the membrane, bilayer thickness decreases and area per lipid increases, indicating disorder in the membrane [10,11]. Bilayer thickness was found to decrease with the increase in the concentration of IL [10]. Small-angle X-ray scattering (SAXS) results also supported the fact that due to incorporation of IL, bilayer thickness was found to decrease [12]. Effects of long alkyl-chain imidazolium-based ILs on the physicochemical properties of the phospholipid membrane have been investigated using dynamics light scattering, transmission electron microscope and fluorescence polarization techniques [21]. It was found that addition of ILs into the phospholipid membrane significantly altered zeta potential, size of the vesicles, fluidity of membrane and cytotoxicity [21]. Growth of Gram negative bacteria, *Escherichia coli* (*E. coli*) in the presence of ILs have also been studied [10]. Bacterial growth was found to be significantly hindered due to incorporation of IL. The efficiency of bacterial inhibition was found to be more at higher concentration of IL. Molecular dynamics (MD) simulations [13-16] have also been carried out to get microscopic insights on the interaction between IL and membrane. Recently, Yoo et al [13] have carried out MD simulation on phosphatidylcholine membrane with imidazolium-based ILs having different alkyl chain length cations. It was found that cations of IL are incorporated spontaneously into the lipid bilayer regardless of the alkyl chain length and stay at a favourable orientation in the membrane. Simulations have also been carried out on different counter anions with varying degree of hydrophobicity. It was found that due to insertion of alkyl chain cations and hydrophobic anions, free energy of the system decreases. Recent studies [14,15] have suggested that inability of some ILs to diffuse from the outer leaflet to the inner leaflet of the phospholipid bilayer could be the prime reason of higher cytotoxicity of IL having longer alkyl chain length [14,15]. Effects of ILs on the structural and dynamical behaviour of membrane have also been studied using MD simulation [16]. It was found that cation of the IL adsorbed into the bilayer, favours penetration of water into the membrane that causes a bilayer thinning. However, no clear trend on the effects of IL on the lipid mobility has been established.

Effects of ILs on the structure have been studied in details [10-12] but not much of information is available on the effects of IL on the dynamical behaviour of the membrane. Membrane dynamics play a key role in the fluidity, stability and viscoelastic behaviour of the

membrane and is a prime determinant in a number of physiological processes, such as cell signaling, membrane trafficking, cell division, fusion, permeability, etc. Any subtle change in the dynamical properties caused by ILs can significantly affect the stability of the cell. Hence, it is of our key interest to investigate effects of ILs on dynamical properties of the membrane. Dynamics of membrane can be studied using various experimental techniques, viz. nuclear magnetic resonance (NMR) [22-23], fluorescence correlation spectroscopy (FCS) [24,25], fluorescence recovery after photo bleaching [26] and quasielastic neutron scattering (QENS) techniques [27-36]. However, most of these techniques are only capable of observing the dynamics on a limited time and length scale. QENS is a suitable technique to study the dynamics of lipid membranes on picoseconds to nanoseconds time scale and on a length scale from angstroms to tens of nanometers [27-36]. Being a scattering technique, QENS provides both spatial as well as temporal information of the dynamics. We have successfully used QENS to study dynamics of surfactant/lipid based self assembled aggregates earlier [29-31, 37-41]. Both qualitative and quantitative information can be extracted through QENS. Qualitative information refers to the geometrical mechanism of the motion, while quantitative information relates to the correlation times and length scales of the motion.

Here, we report the effects of two imidazolium based ILs, namely, BMIM[BF<sub>4</sub>] and DMIM[BF<sub>4</sub>] on the nanoscopic dynamics and phase behaviour of DMPC membrane as studied using fixed elastic window scan (FEWS) and QENS techniques. The pressure-area isotherms were also measured to investigate the interactions of ILs with the self-assembled lipid monolayer. QENS measurements have been carried out on DMPC membrane with and without BMIM[BF<sub>4</sub>] and DMIM[BF<sub>4</sub>] ILs at different temperatures to investigate dependence of phase state of the membrane.

## Experimental Methods

### Preparation of Unilamellar Vesicles

DMPC lipid powder, BMIM[BF<sub>4</sub>], DMIM[BF<sub>4</sub>] ILs and D<sub>2</sub>O (99.9%) were purchased from Sigma Aldrich (USA). Unilamellar vesicles of DMPC were prepared using the method as described by us earlier [29-31]. In brief, required amount of DMPC powder was taken in a glass vial and co-dissolved in chloroform, which results a transparent solution. Chloroform was evaporated using the gentle stream of nitrogen gas to obtain films of DMPC. To remove the residual organic solvent, the lipid films were dried by placing the samples under vacuum

( $10^{-3}$  atm) for about 10 hrs at 320 K. Dry lipid films were suspended in the desired amount of  $D_2O$  at 320 K and vortex mixed for  $\sim 15$  minutes. The vortexed solutions were then exposed to a set of three freeze-thaw cycles by alternately placing the lipid suspension in a warm water bath (330 K) and in a freezer (253 K). Unilamellar vesicles were prepared by extrusion method in which lipid suspension went through a mini-extruder (from Avanti Polar Lipids) fitted with a Whatman® Nuclepore Track-Etched Membrane having average pore diameter of 100 nm. The extrusion was performed in sets of 21 passes, to obtain unilamellar vesicles. During the extrusion process, the temperature of extruder was kept at  $\sim 320$  K to ensure that DMPC lipids were in the fluid phase. To incorporate BMIM[BF<sub>4</sub>] and DMIM[BF<sub>4</sub>] ILs into membranes, 20 mol % of each ILs was added to the vesicles solution at 320 K and mixed well. This mixture was kept at 310K for about 2 hrs for equilibration and then used for experiments.

### Neutron Scattering Experiments

Fixed Elastic window scan (FEWS) and QENS experiments have been carried out on 100mM DMPC membrane in absence and presence of 20mM BMIM[BF<sub>4</sub>] and DMIM[BF<sub>4</sub>] ILs using the near-backscattering spectrometer DNA [42] at MLF, J-PARC, Japan. The final energy was 2.084 meV with the Si(111) analyzer array. In the used configuration, spectrometer has an energy resolution (FWHM) of 3.6  $\mu$ eV and the available energy transfer range of - 40 to 100  $\mu$ eV. The available  $Q$  range was 0.13 to 1.88  $\text{\AA}^{-1}$ . FEWS experiments on DMPC membrane with and without IL have been carried out from 9 to 37°C in the heating cycle with a rate of 0.25° C /min. To check the reversibility of the transition, FEWS experiments have also been carried out in the cooling cycle. QENS experiments have been carried out on DMPC membrane with and without BMIM[BF<sub>4</sub>] and DMIM[BF<sub>4</sub>] at three distinct temperatures 10, 20 and 30°C . To make a meaningful comparison between the two ILs, all experimental conditions, such as molar concentration of IL, temperature, etc. were kept same. QENS data have also recorded from pure  $D_2O$  at the same temperatures as a reference. To obtain the instrumental resolution, QENS measurements were performed on standard vanadium sample. For neutron scattering experiments, samples were placed in an annular aluminium double cylindrical sample holders with 1 mm internal spacing with the outer diameter is 14.0 mm, the inner diameter is 12.0 mm. and the effective length is about 40 mm. The sample thickness was chosen such that no more than 10% scattering from the samples, thereby minimizing multiple scattering effects.

## Differential Scanning Calorimetry (DSC) Measurements

DSC experiments were carried out on DMPC vesicles with and without 20 mol% DMIM[BF<sub>4</sub>] using a NANO DSC Series III System with Platinum Capillary Cell (TA Instruments). The thermograms were recorded for both heating and cooling cycle for each vesicles solution with a scan rate of 0.5 °C /min in the temperature range of 5-40°C.

## Monolayer Isotherm Measurements

The pressure-area isotherm of DMPC was constructed using a Langmuir trough of size 55×15×0.5 cm<sup>3</sup> (APEX, Kolkata, India). The lipid with and without 20 mol% ILs were dissolved in common solvent chloroform with a concentration of 0.5 mg/ml of DMPC and about 125 µl of the solution was spread on deionized water of specific resistivity of 18 MΩ cm (Millipore). After 15 min of waiting, the double barriers were compressed symmetrically at a speed of 5 mm/min. The interaction of the ILs with the lipids was monitored by the modified isotherm of the lipid in the presence of 20 mol% of the ILs into the monolayer forming molecular mixtures. All the measurements were performed at pH 7.4 and temperature at 20°C.

## Results and Discussion

The pressure ( $\pi$ )-area (A) isotherm measurement of Langmuir monolayer is a simple technique to follow the interaction of any foreign macromolecules with the self-assembled lipid monolayer formed at air-water interface [43]. As shown in Fig. 2 (a), the presence of 20 mol% of ILs in the monolayer forming lipid solutions have considerable effect on the phase behaviour of pure DMPC. Even though the decrease of collapse-pressure of isotherms is not affected much by the presence of ILs, the isotherms shift towards the higher area-per lipid molecule exhibiting the penetration of the molecules into the lipid monolayer. It is evident that DMIM[BF<sub>4</sub>] has stronger effect compared to BMIM[BF<sub>4</sub>]. At lower pressure, 15 mN/m, the area/lipid changes from 53.5 Å<sup>2</sup> to 63.2 Å<sup>2</sup> (increase of 18 %) after adding DMIM[BF<sub>4</sub>] whereas the value goes to 57.04 Å<sup>2</sup> (increase of 6.5 %) for BMIM[BF<sub>4</sub>]. At higher surface pressure, 30mN/m, the change in area/lipid is found to be 9.3 % and 2.6% for DMIM[BF<sub>4</sub>] and BMIM[BF<sub>4</sub>], respectively. Both ILs have the same head group and counterion, hence their electrostatic effects on the self-assembled monolayer of the lipid is expected to be the same. However, the steric repulsion due to alkyl chains should be very different as the chain lengths are distinctly different. As mentioned earlier, BMIM[BF<sub>4</sub>] has four carbons in its

alkyl chain and DMIM[BF<sub>4</sub>] has ten. As the amount of both ILs is same here, the stronger lateral ‘push’ from longer chain in DMIM[BF<sub>4</sub>] could provide higher effective surface area for a lipid molecule.

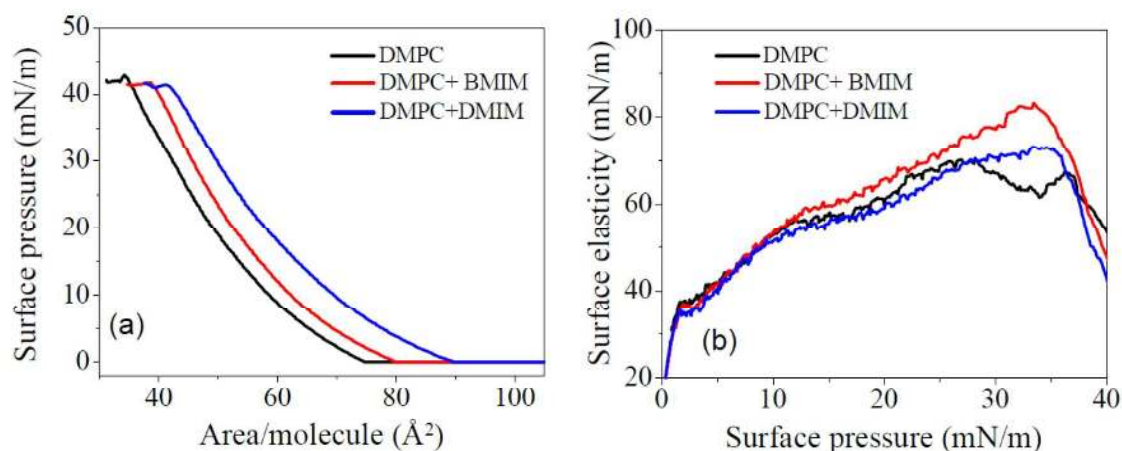


**Fig. 2** (a) Pressure-area isotherm of DMPC monolayers with and without ILs. (b) The in-plane elasticity of the monolayers calculated from the respective isotherms.

The in-plane surface elasticity ( $\beta^{-1}$ ) of each layer has been calculated using,  $\beta^{-1} = -A \left( \frac{\delta\pi}{\delta A} \right)_T$  where  $\beta$  is the two-dimensional isothermal compressibility. At lower surface pressure, the presence of both the ILs do not show considerable change in the in-plane elasticity, however, the changes become prominent at higher surface pressure [Fig. 2(b)]. At 30 mN/m, the in-plane elasticity changes from 67.1 mN/m for pure DMPC to 77.5 mN/m for DMPC with BMIM[BF<sub>4</sub>], whereas it is found to be 70.8 mN/m for DMPC with DMIM[BF<sub>4</sub>]. As stated above, the effects on the conformation of the lipid chain are expected to be very different for these two ILs having different alkyl chain lengths. This, in turn, may affect the in-plane elasticity differently.

FEWS or elastic intensity scan is very useful to study the existence of phase transition in the sample related to the dynamics, by measuring the elastic scattering intensity within the energy resolution of the spectrometer as a function of temperature. Any abrupt change in elastic intensity is a signature of a phase transition associated with an alteration in the microscopic dynamics at that temperature. FEWS experiments have been carried out on DMPC membrane with and without ILs in heating as well as in cooling cycles. The  $Q$  averaged ( $0.32 \text{ \AA}^{-1}$  to  $1.88 \text{ \AA}^{-1}$ ) elastic scans are shown in the Fig.3. In the heating cycle (Fig. 3(a)), for pure DMPC membrane, it is evident that elastic intensity decreases with the

increase in the temperature and a sharp fall in elastic intensity is observed at 24°C. It is known that DMPC membrane undergoes main phase transition (solid gel to fluid) at 24°C [44]. Hence, this sudden fall at 24°C should correspond to the main phase transition of DMPC membrane. However, in presence of ILs, elastic intensity scan is found to be affected and main phase transition shifts to the lower temperature. In addition, our data show that interaction between membrane and IL strongly depends on the alkyl chain length of IL's cation and found to be stronger with the longer chain length. For example, for BMIM (shorter chain length) the main phase transition shifts about 2°C. However, for DMIM (longer chain length), it is found to shift about 6°C. In the cooling cycle (Fig 3(b)), elastic intensity scan for DMPC membrane with and without ILs are observed to be similar to the elastic scans in the heating cycle indicating reversibility of the transitions for membrane with and without ILs. DSC measurements have been carried out on DMPC membrane with and without DMIM[BF<sub>4</sub>] in heating and cooling cycles and the obtained thermograms are shown in Fig 3(c). DMPC membrane shows a sharp peak at ~ 24°C which corresponds to the main phase transition. It is found that due to incorporation of DMIM[BF<sub>4</sub>], this peak is shifted towards lower temperature and gets broadened which is consistent with our elastic intensity scan measurements.

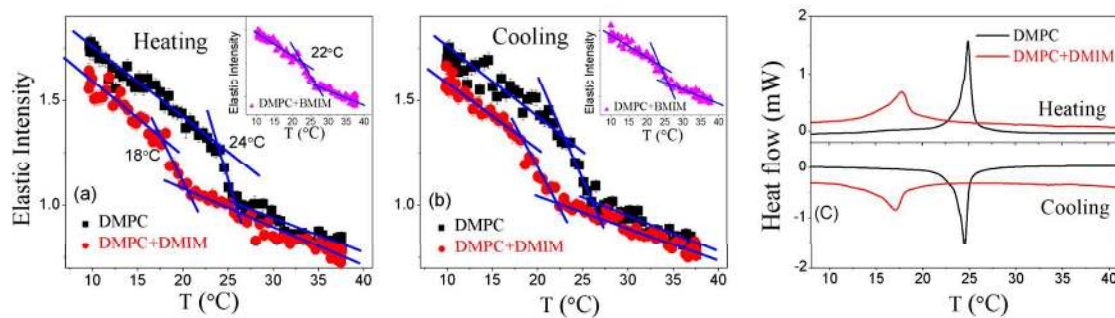


**Fig. 3**  $Q$ -averaged ( $0.32 \leq Q \text{ (\AA}^{-1}) \leq 1.88$ ) FEWS for the DMPC membrane with and without DMIM[BF<sub>4</sub>] during (a) heating and (b) cooling cycles. The same for the DMPC membrane with BMIM[BF<sub>4</sub>] are shown in the inset. Solid lines are drawn as guide to the eyes. (c) DSC thermograms of DMPC membrane with and without DMIM[BF<sub>4</sub>] in heating and cooling cycles.

To get detailed insights on the effects of ILs on the dynamical behaviour of the membrane, QENS experiments have been carried out on DMPC membrane with and without

BMIM[BF<sub>4</sub>] and DMIM[BF<sub>4</sub>] at 10°C, 20°C and 30°C. At 10°C and 20°C, pure DMPC membrane is in ordered phase whereas at 30°C, it is in the fluid phase. QENS spectra have also been recorded on pure D<sub>2</sub>O (solvent) and subtracted from the spectra of the vesicle solutions. The scattered intensity from the membrane,  $I_{mem}(Q, \omega)$ , can be obtained as,

$$I_{mem}(Q, \omega) = I_{solution}(Q, \omega) - \phi I_{D_2O}(Q, \omega) \quad (1)$$

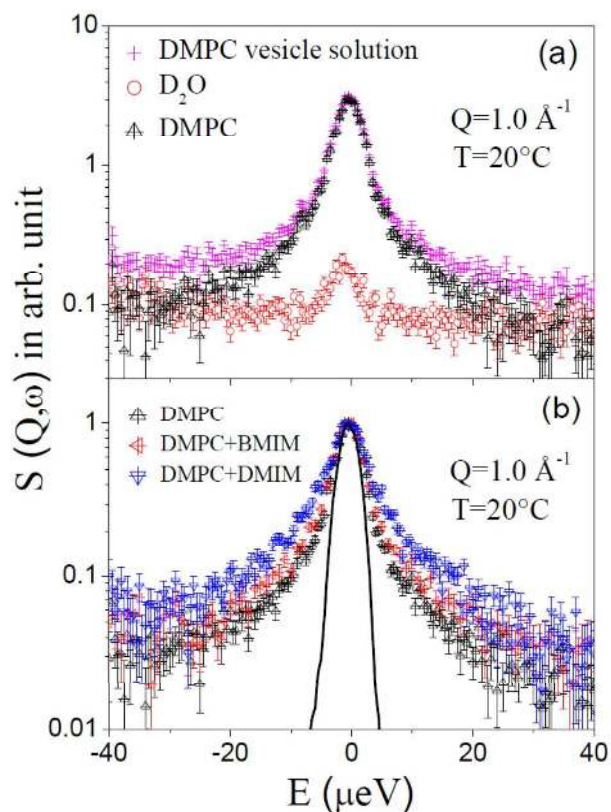


**Fig. 4** Typical measured QENS spectra at  $Q=1.0 \text{ \AA}^{-1}$  and  $T=20^\circ\text{C}$  for (a) DMPC vesicles solution, solvent D<sub>2</sub>O and DMPC membrane (after subtracting the contribution of D<sub>2</sub>O) (b) A relative comparison of QENS spectra for DMPC membrane with and without BMIM[BF<sub>4</sub>] and DMIM[BF<sub>4</sub>] ILs. The contribution of the solvent (D<sub>2</sub>O) has been subtracted, and the resultant spectra are normalized to the peak amplitudes. Instrument resolution is shown by a solid line.

where  $\phi$  is the volume fraction of D<sub>2</sub>O. Typical measured QENS spectra for DMPC vesicles solution and solvent (D<sub>2</sub>O) at 20°C at a typical  $Q$  value of  $1.0 \text{ \AA}^{-1}$  are shown in Fig.4 (a).

Solvent contribution has been subtracted using Eq. (1) and resultant subtracted spectra for DMPC membrane at 20°C is also shown. Subtracted QENS spectra for DMPC membrane with and without BMIM[BF<sub>4</sub>] and DMIM[BF<sub>4</sub>] ILs at 20°C are shown in Fig. 4(b). Contribution of the ILs in the signal is very small and hence not considered. It may be noted that BMIM[BF<sub>4</sub>] and DMIM[BF<sub>4</sub>] ILs contribute about 4 and 7 % of the total incoherent scattering signal, respectively. Instrument resolution as measured from standard vanadium sample is also shown in Fig 4(b). For direct comparison, spectra are normalised to peak amplitude. Significant quasielastic (QE) broadening is observed for DMPC membrane with and without ILs indicating presence of stochastic motion of the lipid molecules. It is evident from Fig. 4 that addition of ILs into the DMPC membrane, leads to increase in the QE broadening. DMIM[BF<sub>4</sub>] is found to affect the dynamics of membrane more in comparison with BMIM[BF<sub>4</sub>], indicating that interaction between IL and phospholipid membrane depends on the chain length of the cation of IL.

Lipid molecules can undergo different kinds of motion including vibrational, rotational, lateral, flip flop, encompassing a broad range of time scales from femto seconds for molecular vibrations, to a few minutes for the trans-bilayer flip flop. High energy resolution DNA spectrometer ( $\Delta E \sim 3.6 \mu\text{eV}$ ) is a well suited spectrometer to study lateral ( $\sim\text{ns}$ ) and internal motions ( $\sim\text{ps}$ ) of the lipid, which is of our current interest. Assuming both motions are independent of each other, scattering law for the membrane can be written as

$$S_{mem}(Q, \omega) = S_{lat}(Q, \omega) \otimes S_{int}(Q, \omega) \quad (2)$$

where  $S_{lat}(Q, \omega)$  and  $S_{int}(Q, \omega)$  are the scattering functions corresponding to lateral and internal motions of the lipid molecules, respectively. The lateral motion of lipids is expected to be characterized by continuous diffusion [29-31], which is described by a Lorentzian scattering law

$$S_{lat}(Q, \omega) = L_{lat}(\Gamma(Q), \omega) = \frac{1}{\pi} \frac{\Gamma_{lat}}{\Gamma_{lat}^2 + \omega^2} \quad (3)$$

where  $\Gamma_{lat}$  is the half width at half-maximum (HWHM) of the Lorentzian corresponding to the lateral motion of the lipid molecule.

The internal motion of lipids is instead localized in nature, so there exists a finite probability of finding the hydrogen atoms within the volume of the lipid even after a sufficiently long time. This in turn gives rise to an elastic contribution in the scattering law.

Thus, the scattering law for internal motions can be written as a linear combination of an elastic component and a Lorentzian function [27,29]

$$S_{\text{int}}(Q, \omega) = A(Q)\delta(\omega) + (1 - A(Q))L_{\text{int}}(\Gamma_{\text{int}}, \omega) \quad (4)$$

where  $A(Q)$  is Elastic Incoherent Structure Factor (EISF) and  $\Gamma_{\text{int}}$  is the HWHM of the Lorentzian corresponding to the internal motion. Hence, the total scattering law for the membrane can be written as

$$S_{\text{mem}}(Q, \omega) = [A(Q)L_{\text{lat}}(\Gamma_{\text{lat}}, \omega) + (1 - A(Q))L_{\text{tot}}(\Gamma_{\text{lat}} + \Gamma_{\text{int}}, \omega)] \quad (5)$$

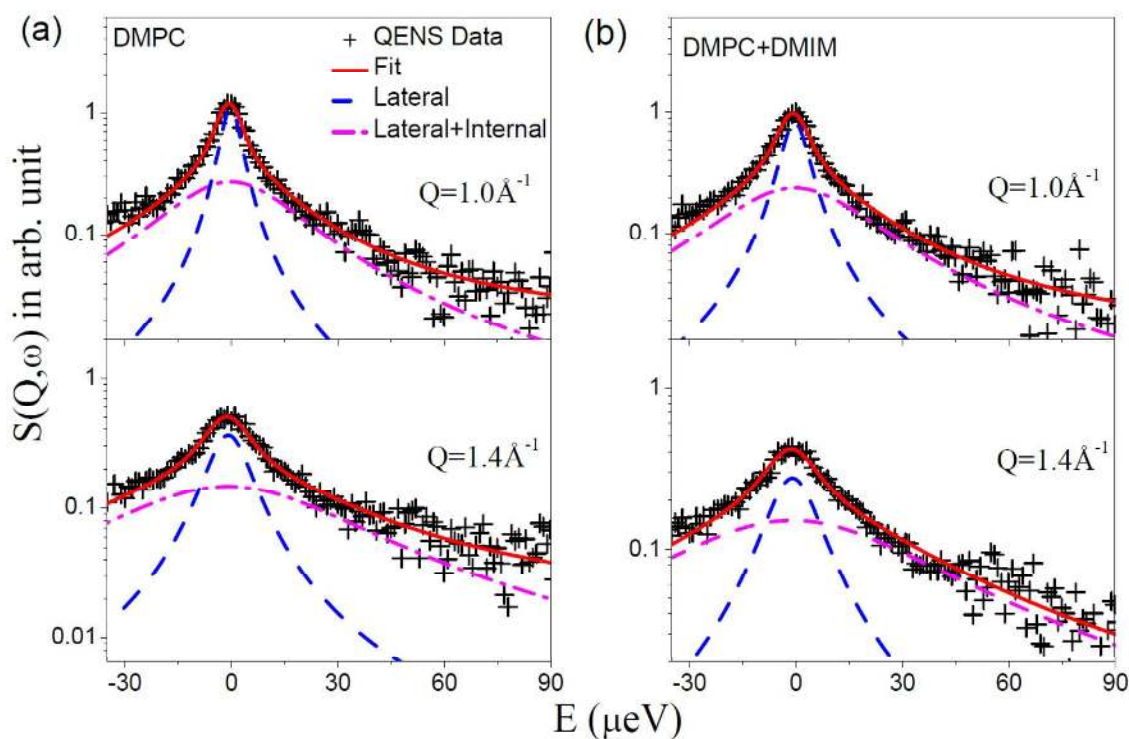


**Fig. 5** Typical fitted QENS spectra for DMPC membrane (a) pure (b) with DMIM[BF4] at 30°C at two different  $Q$  values.

Convoluting Eq. (5) with the resolution function, the parameters  $A(Q)$ ,  $\Gamma_{\text{lat}}$  and  $\Gamma_{\text{int}}$  are determined by the least squares fitting of the measured spectra. DAVE software [45] developed at the NIST Center for Neutron Research has been used for QENS data analysis. It is found that above scattering law describes the QENS spectra for DMPC membrane with and without ILs quite well at all the measured temperatures and  $Q$  values. Typical fitted spectra

for DMPC membrane with and without DMIM[BF<sub>4</sub>] IL at 30°C are shown in Fig. 5. To gain more insight into the two dynamical processes, the parameters obtained from the fit are analyzed as a function of  $Q$ .

### Lateral Motion

The lateral motion of lipid is of paramount interest due to its major role in various biophysical processes, such as cell signaling, membrane trafficking, permeability and so forth. Variations of HWHM of the Lorentzian corresponding to the lateral motion,  $\Gamma_{\text{lat}}$  for DMPC membrane with and without BMIM[BF<sub>4</sub>] and DMIM[BF<sub>4</sub>] at 10, 20 and 30°C are shown in Fig. 6(a). It is found that  $\Gamma_{\text{lat}}$  for all the samples, increases linearly with  $Q^2$ , passing through the origin, which indicates that lateral motion of lipid molecule undergoes continuous diffusion, described by Fick's law,  $\Gamma_{\text{lat}} = D_{\text{lat}}Q^2$ . The lateral diffusion coefficients,  $D_{\text{lat}}$  as obtained from the fit at different temperatures for DMPC membrane with and without ILs are shown in Fig. 6(b). It is evident that incorporation of DMIM[BF<sub>4</sub>] accelerates the lateral motion of the lipid molecules at all the measured temperatures irrespective of the phase of the pure membrane. For example at 20°C where pure DMPC membrane is in ordered phase,  $D_{\text{lat}}$  increases from  $1.6 \pm 0.1 \times 10^{-7}$  cm<sup>2</sup>/s to  $3.6 \pm 0.2 \times 10^{-7}$  cm<sup>2</sup>/s. At 30°C where pure membrane is in fluid phase,  $D_{\text{lat}}$  of DMPC membrane increases from  $4.8 \pm 0.2 \times 10^{-7}$  cm<sup>2</sup>/s to  $6.6 \pm 0.2 \times 10^{-7}$  cm<sup>2</sup>/s. These results are in contrast with our earlier QENS study on the effects of an archetypal antimicrobial peptide melittin on the dynamics of phospholipid membrane [30]. It was found that interaction of melittin with the membrane strongly depends on the physical state of the membrane. In the fluid phase, it acts as stiffening agent, restricting the dynamics of the membrane. However, in the gel phase, it acts as a plasticizer; enhances the fluidity of the membrane. Our measurements showed that addition of the same amount of BMIM[BF<sub>4</sub>], having shorter chain length cation, does not affect the lateral motion much as compared to DMIM[BF<sub>4</sub>]. Structural studies performed earlier [9] have discussed the dependence of alkyl chain length of the cations on the interaction with cell membrane and found that as the chain length of cation increases, IL perturbs the structure of cell membrane more strongly. Our results are found to be consistent showing that the IL having longer chain length cation, interact more strongly with the cell membrane and enhances the lateral motion of the lipid significantly. As mentioned earlier, modification in dynamics can affect the stability of the cell profoundly and may eventually leads to their death. Hence, observed changes in the dynamical behaviour of the membrane could be correlated with the

antimicrobial actions of the ILs. Lateral diffusion of lipids in membrane depends on various factors [46,47] including area per lipid, binding affinity between additive and lipids, obstructions, etc. In general, factors for direct effect of obstruction and binding affinity between additive and lipids, contribute towards the hindrance of the lateral motion. Reflectivity and SAXS [10-12] studies show that incorporation of IL into membrane creates disorder in the membrane resulting increase in the area per lipid. This is consistent with the pressure area isotherms (Fig. 2(a)), which show that area per lipid molecules increases due to incorporation of the ILs. Hence, increase in area per lipid has the dominant contribution for the observed enhanced diffusivity. In contrast to DMIM[BF<sub>4</sub>], other IL, BMIM[BF<sub>4</sub>], affects the lateral motion of the membrane to the lesser extent compared to DMIM[BF<sub>4</sub>]. This is

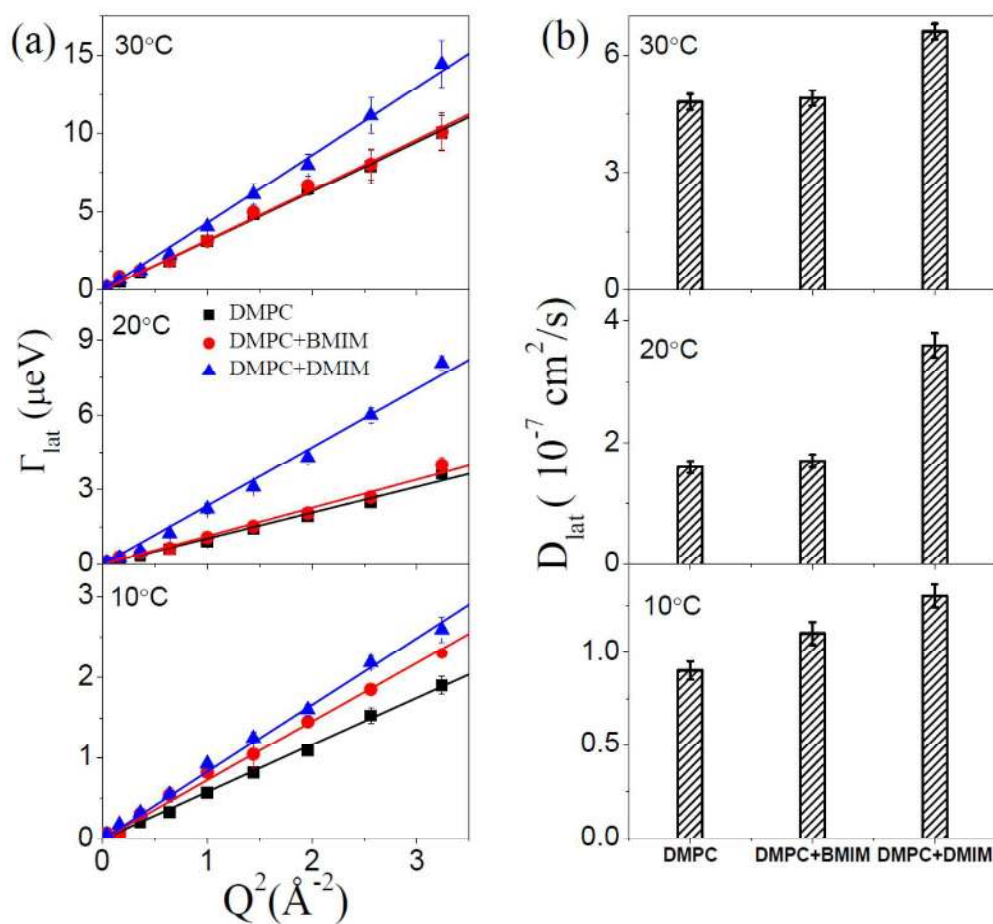


**Fig. 6** (a) Variations of HWHM of the Lorentzian function corresponding to the lateral motion,  $\Gamma_{lat}$  with  $Q^2$  for DMPC membrane with and without ILs at 10°C, 20°C and 30°C. The solid lines are the fits with Fick's law of diffusion. (b) Lateral diffusion coefficient,  $D_{lat}$  for DMPC membrane with and without the ILs.

found to be consistent with the pressure area isotherm which shows that due to addition of BMIM[BF<sub>4</sub>] increase in area per lipid is less compared to DMIM[BF<sub>4</sub>].

### Internal Motion

As mentioned earlier QENS data from DMPC showed presence of internal motion of the lipid in addition to the lateral motion. Internal motions of lipid can be characterised by the elastic incoherent structure factor (EISF),  $A(Q)$  and HWHM,  $\Gamma_{int}$  as described in Eq. (4). EISF and HWHM,  $\Gamma_{int}$ , obtained for DMPC membrane with and without ILs are shown in Figs. 7 and 8 respectively. Internal motion of lipid molecule comprises various motions, including reorientation, conformational like bond bending and stretching, torsional, etc. The superposition of all these motions can be effectively described by assuming that the hydrogen atoms of each CH<sub>2</sub> unit undergo localised translational diffusion (LTD) within a spherical volume. The observed  $Q$  dependence of the EISF and of  $\Gamma_{int}$ , as shown in Figs. 7 and 8, is also indicative of the LTD model. Indeed, in the zero- $Q$  limit,  $\Gamma_{int}$  flattens towards a finite nonzero value and increases with increasing  $Q$ , which is a typical signature of the LTD [48]. Due to flexibility of acyl chain, all of the hydrogen atoms may not have same size of spherical domain and diffusivity. In principle, different distribution functions for the radii and diffusivity may be considered, such as linear, Gaussian, log-normal, etc. We have assumed a linear distribution similar to that used for phospholipid membrane [28,29]. In this model, the least radius and diffusivity is for the CH<sub>2</sub> unit near the head and largest at the tail end. Scattering law for this model can be written as [48]

$$S_{int}(Q, \omega) = \frac{1}{N} \sum_{i=1}^N \left[ \left[ \frac{3j_1(QR_i)}{QR_i} \right]^2 \delta(\omega) + \frac{1}{\pi} \sum_{\{l,n\} \neq \{0,0\}} (2l+1) A_n^l(QR_i) \frac{(x_n^l)^2 D_i / R_i^2}{\left[ (x_n^l)^2 D_i / R_i^2 \right]^2 + \omega^2} \right] \quad (6)$$

The first term in the above equation is the elastic component with the EISF

$$A(Q) = \frac{1}{N} \sum_{i=1}^N \left[ \frac{3j_1(QR_i)}{QR_i} \right]^2 \quad (7)$$

Where  $R_i$  is the radius of the spherical domain of dynamics generated by the CH<sub>2</sub> units at the  $i^{\text{th}}$  site of the acyl chain and for a linear distribution can be written as,

$$R_i = \frac{i-1}{N-1} [R_{\max} - R_{\min}] + R_{\min} \quad (8)$$

$R_{min}$  and  $R_{max}$  are the radii of the smallest and largest spherical domains, respectively.

The second term in Eq. (6) is the quasielastic component with  $A_n^l(QR_i)$  ( $n, l \neq 0,0$ ) is the associated structure factor. Values for  $A_n^l(QR_i)$  for different  $n$  and  $l$  can be calculated by using the values of  $x_n^l$  [48].  $D_i$  is the diffusivity associated with the CH<sub>2</sub> units at the  $i^{\text{th}}$  site of the acyl chain from the polar head towards tail, and can be expressed as,

$$D_i = \frac{i-1}{N-1} [D_{max} - D_{min}] + D_{min} \quad (9)$$

where  $D_{min}$  and  $D_{max}$  are the minimum and maximum diffusion coefficients, respectively and  $N$  is the total number of CH<sub>2</sub> units in the acyl chain. For DMPC,  $N$  equals to 14.

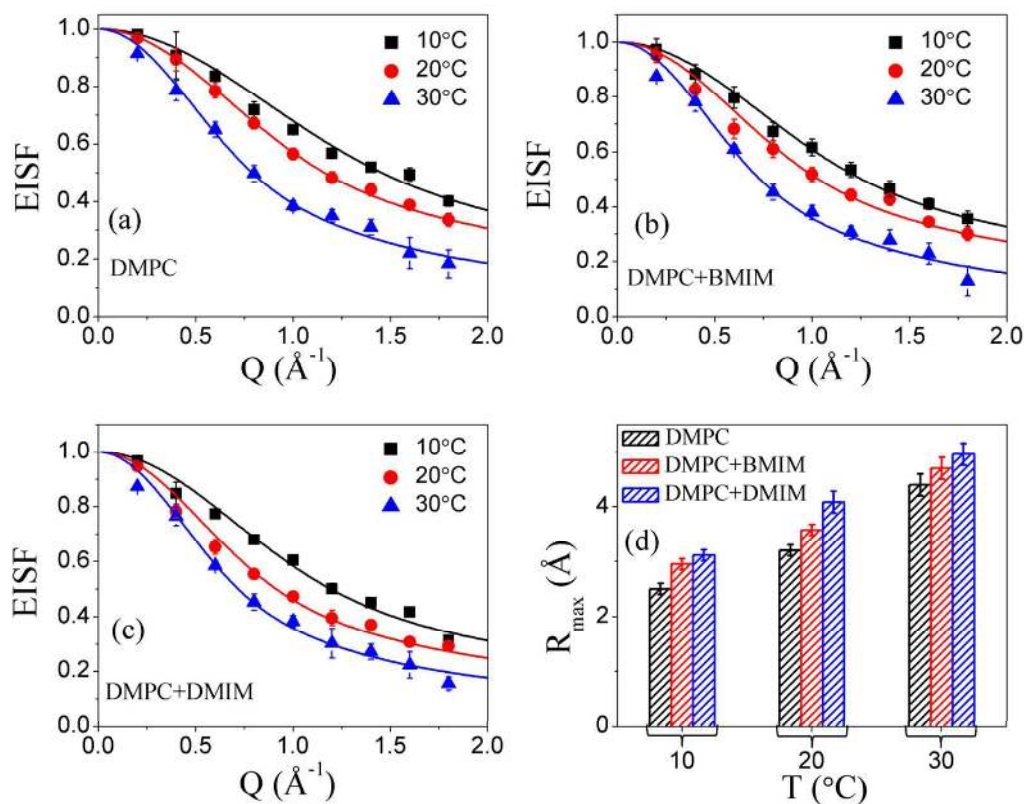


**Fig. 7** Variations of EISF for DMPC membrane (a) pure with (b) BMIM[BF<sub>4</sub>] and (c) DMIM[BF<sub>4</sub>] ionic liquids at 10°C, 20°C and 30°C. Solid lines are the EISF as per the localised translational diffusion model described in text. (d) Values of  $R_{max}$  for pure DMPC membrane and in the presence of ionic liquids at different temperatures.

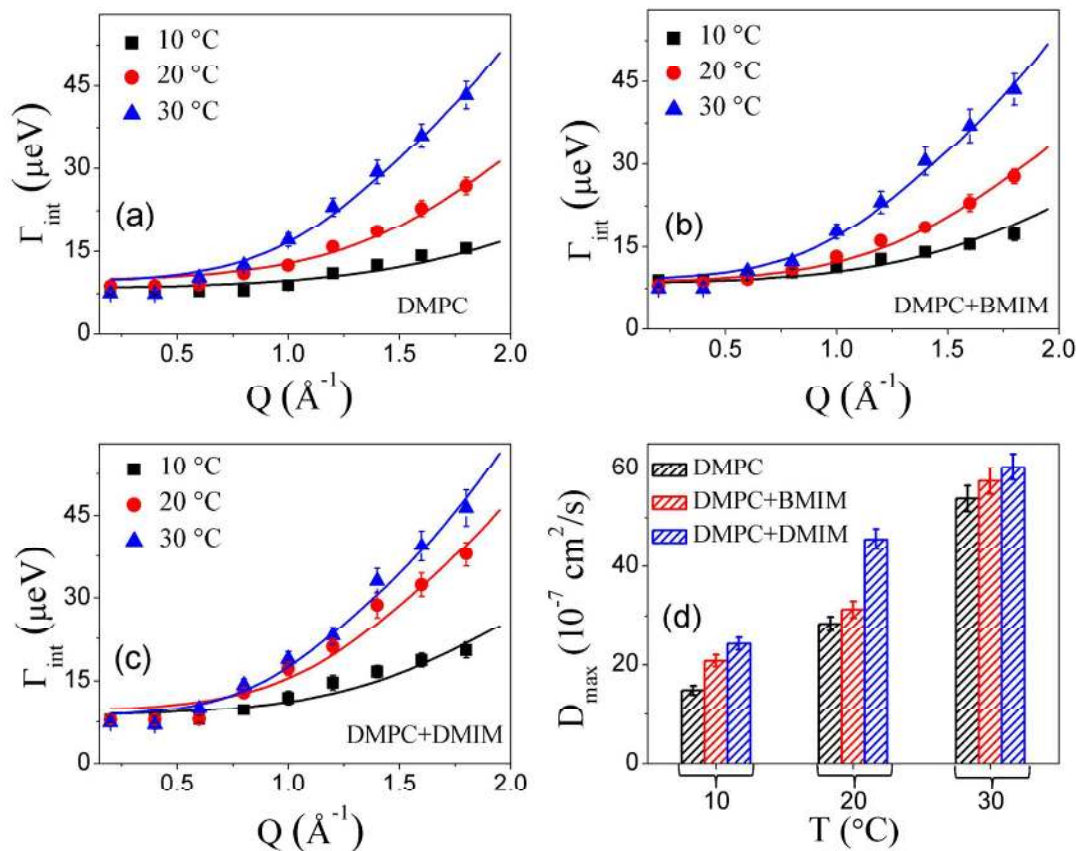


**Fig. 8** Variation of HWHM corresponding to internal motion of DMPC membrane (a) pure with (b) BMIM[BF<sub>4</sub>] and (c) DMIM[BF<sub>4</sub>] at 10°C, 20°C and 30°C. Solid lines are the fits according to localised translational diffusion as described in the text. (d) Variation of  $D_{\text{max}}$  with temperature for pure DMPC membrane and in the presence of the ILs.

Least squares fitting method has been used to describe the observed EISF using Eqs. (7) and (8) with  $R_{\text{min}}$  and  $R_{\text{max}}$  as the fitting parameters. It is found that the LTD model describes the observed EISF quite well for DMPC membrane with and without the ILs at all the measured temperatures as shown by solid lines in Fig. 7 (a-c). The sizes of spherical volumes ( $R_{\text{min}}$  and  $R_{\text{max}}$ ) are obtained from the least square fits. The values of  $R_{\text{min}}$  are found to be insignificantly small and could only reflect the negligible movement of the hydrogens in the first carbon position nearest to the head group. Obtained values of  $R_{\text{max}}$  for DMPC membrane in pure and in presence of the ILs at different temperatures are shown in Fig. 7 (d). It is evident that as the temperature increases, values of  $R_{\text{max}}$  increase for all DMPC membranes (with and without ILs) indicating more flexibility of the acyl chain at higher

temperatures. It is of interest to compare the value of  $R_{max}$  for pure DMPC membrane and in presence of ILs at the same temperature. It is found that incorporation of both ILs make lipid molecule more flexible as size of confining spheres increases at all the measured temperatures irrespective of the physical state of the pure membrane. Unlike lateral motion, BMIM[BF<sub>4</sub>] is also found to affect the internal motion significantly. Increase in  $R_{max}$  depends on the alkyl chain length and found to be higher for DMIM[BF<sub>4</sub>] which has longer alkyl chain length. For example, at 20°C, for pure DMPC membrane  $R_{max}$  is found to be  $3.2 \pm 0.1$  Å which increases to  $3.6 \pm 0.1$  Å for DMPC with BMIM[BF<sub>4</sub>] and to  $4.1 \pm 0.2$  Å for DMPC with DMIM[BF<sub>4</sub>].

Unlike EISF, there is no analytical expression for the HWHM of the quasielastic part for the LTD model. However, one can calculate it numerically for given values of  $R_{min}$ ,  $R_{max}$ ,  $D_{min}$  and  $D_{max}$  using Eqs. 6 to 9. The least squares fitting method is used to describe the observed quasielastic width corresponding to the internal motion with  $D_{min}$  and  $D_{max}$  as parameters, while the values of  $R_{min}$  and  $R_{max}$  are already known from the fits of the EISF. It is found that LTD model described the variation of HWHM quite well for DMPC membrane with and without ILs at all the measured temperatures. The solid lines in Fig. 8(a-c) represent the fits as per the LTD model. Values of  $D_{min}$ , like  $R_{min}$ , are found to be insignificantly small and hence not discussed here. Obtained values of  $D_{max}$  for DMPC membrane in pure and in presence of ILs are shown in Fig. 8 (d) at different temperatures. As expected,  $D_{max}$  increases for all DMPC membranes as temperature increases. It is found that incorporation of ILs, significantly affect the diffusivity corresponding to internal motion. Our measurements show that the internal motion of lipid becomes faster due to addition of IL. The change in the diffusivity depends on the alkyl chain length of the IL and found to be higher for IL having longer alkyl chain length i.e. DMIM[BF<sub>4</sub>]. For example, at 10°C,  $D_{max}$  for pure DMPC membrane is found to be  $14.9 \pm 0.9 \times 10^{-7}$  cm<sup>2</sup>/s which is  $20.8 \pm 1.2 \times 10^{-7}$  cm<sup>2</sup>/s for DMPC with BMIM[BF<sub>4</sub>] and  $24.2 \pm 1.2 \times 10^{-7}$  cm<sup>2</sup>/s for DMPC with DMIM[BF<sub>4</sub>]. These results indicate that DMIM[BF<sub>4</sub>] affects both long range lateral and localised internal motions of the membrane, whereas BMIM[BF<sub>4</sub>] affects mainly the localised internal motion.

In summary, effects of two imidazolium based room temperature ILs with different alkyl chain lengths on the dynamics and phase behaviour of DMPC phospholipid membrane have been studied. The pressure-area isotherm measurements show that incorporation of ILs shift isotherms towards the higher area-per lipid molecules. FEWS shows that incorporation of ILs has profound effects on the phase behaviour of the phospholipid membrane; main

phase transition gets shifted towards the lower temperature. Results are found to be consistent with the calorimetric measurements. It is found that effect of IL on the phase behaviour of the membrane depends on the alkyl chain length of IL. DMIM[BF<sub>4</sub>] is found to affect the phase behaviour more strongly in comparison to BMIM[BF<sub>4</sub>], which has shorter alkyl chain length. QENS data analysis indicates two distinct motions namely lateral and internal motions of the lipids. Our measurements suggest that both motions are found to be altered due to incorporation of ILs. Both ILs act as a plasticizer and incorporation of these enhance the dynamics of the membrane irrespective of the physical state of the pure membrane i.e in ordered as well as in fluid phase. It is found that in comparison to BMIM[BF<sub>4</sub>], DMIM[BF<sub>4</sub>] acts more strongly on the phospholipid membrane and creates disorder in the membrane which results in higher lateral as well as internal diffusivity. However, BMIM[BF<sub>4</sub>] affects mainly towards localised internal motion. Results are found to be correlated with the dependence of antimicrobial activity with the chain length [17]. For the environmental point of view, microscopic understanding of the cytotoxicity mechanism of ILs can be helpful in the designing of nontoxic ILs. For example, our study shows that effects of ILs on the dynamical and phase behaviour of membrane is higher with IL having longer alkyl chain length and found to be correlated with the cytotoxicity of IL. Hence, branched IL would be preferable for non toxicity rather than IL having longer alkyl chain length.

### Conclusions

Imidazolium based ionic liquids, 1-butyl-3-methylimidazolium tetrafluoroborate (BMIM[BF<sub>4</sub>]) and 1-decyl-3-methylimidazolium tetrafluoroborate (DMIM [BF<sub>4</sub>]) are found to affect the microscopic dynamics and the phase behaviour of the DMPC membrane significantly. The two ILs considered here differ only in terms of alkyl chain length of the cation. Neutron scattering measurements showed that incorporation of ILs into the DMPC membrane significantly affect the phase behaviour of the membrane and creates disorder in the membrane. Main phase transition not only shifted towards the lower temperature but also gets broadened, which is consistent with the calorimetric measurements. It is found that ILs acts as plasticizer which enhances, in general, both the long range lateral and localised internal motions in the ordered as well as in fluid phases. DMIM[BF<sub>4</sub>], which has cation of longer alkyl chain, is found to affect the dynamics and phase behaviour of membrane more strongly in comparison to BMIM[BF<sub>4</sub>]. Results are found to be consistent with monolayer isotherm measurements which indicates that increase in area/lipid due to addition of DMIM[BF<sub>4</sub>] is more compared to BMIM[BF<sub>4</sub>]. It is found that DMIM[BF<sub>4</sub>] enhances both

the lateral and internal motions whereas BMIM[BF<sub>4</sub>] does not affect the later motion much but internal motion is stimulated. In conjunction with earlier studies, which showed that toxicity of IL towards bacteria increases with the chain length, our study provides evidence that interaction of IL with the cell membrane could be the prime reason of their antimicrobial activity. Present study provides microscopic insights on the interaction of ILs with the model cell membrane which is useful for the design of greener and safer ILs.

### Acknowledgements

The QENS experiments using DNA spectrometer in BL02 at the Materials and Life Science Experimental Facility of the J-PARC was carried out under the user program organized by J-PARC Center and CROSS-Tokai (Proposal No. 2017A0076). RM is thankful to Prof. T. Kanaya and Dr. Y. Kawakita for very useful discussion. R. Mukhopadhyay would like to thank the Department of Atomic Energy, India, for the award of Raja Ramanna Fellowship.

## References

1. R. Hayes, G. G. Warr and R. Atkin, *Chem. Rev.*, 2015, **115** (13), 6357–6426.
2. K. M. Docherty and C. F. Kulpa Jr, *Green Chem.*, 2005, **7**, 185–189.
3. N. V. Plechkova and K. R. Seddon, *Chem. Soc. Rev.*, 2008, **37** (1), 123–150.
4. J. Lu, F. Yan, and J. Texter, *Prog. Polym. Sci.*, 2009, **34** (5), 431–448.
5. J. S. Wilkes, *J. Mol. Catal. A: Chem.*, 2004, **214** (1), 11–17.
6. F. Ganske and U. T. Bornscheuer, *Biotechnol. Lett.*, 2006, **28**, 465–469.
7. T. P. T. Pham, C.W. Cho and Y. S. Yun, *Water Research*, 2010, **44**, 352–372.
8. A. Latała, M. Nędzi and P. Stepnowski, *Green Chem.*, 2009, **11**, 1371–1376.
9. S. Jeong, S. H. Ha, S. H. Han, M.C. Lim, S. M. Kim, Y. R. Kim, Y. M. Koo, J. S. Soa and T.J. Jeon, *Soft Matter*, 2012, **8**, 5501–5506.
10. G. Bhattacharya, R. P. Giri, H. Saxena, V. V. Agrawal, A. Gupta, M. K. Mukhopadhyay, and S. K. Ghosh, *Langmuir* 2017, **33**, 1295–1304.
11. A. Benedetto, F. Heinrich, M. A. Gonzalez, G. Fragneto, E. Watkins, and P. Ballone, *J. Phys. Chem. B*, 2014, **118**, 12192–12206.
12. I. Kontro, K. Svedström, F. Duša, P. Ahvenainen, S. K. Ruokonen, J. Witos and S. K. Wiedmer, *Chem Phys Lipids*, 2016, **201**, 59–66.
13. B. Yoo, J. K. Shah, Y. Zhu and E. J. Maginn, *Soft Matter*, 2014, **10**, 8641–8651.
14. B. Yoo, Y. Zhu and E. J. Maginn, *Langmuir*, 2016, **32**, 5403–5411.
15. B. Yoo, B. Jing, S. E. Jones, G. A. Lamberti, Y. Zhu, J. K. Shah, E. J. Maginn, *Scientific Reports*, 2016, **6**, 19889.
16. A. Benedetto, R. J. Bingham, P. Ballone, *J. Chem. Phys.*, 2015, **142**, 124706.
17. Y. Yu, and Y. Nie, *J. Environ. Prot.*, 2011, **2** (03), 298.
18. J. N. Pendleton, B. F. Gilmore, *International Journal of Antimicrobial Agents*, 2015, **46**, 131–139.
19. D. M. Engelman, *Nature*, 2005, **438**, 578–580.
20. M. Eeman and M. Deleu, *Biotechnol Agron Soc Environ*, 2010, **14**, 719–36.
21. C. H. Liang, W.Y. Ho, L.H. Yeha, Y. S. Chenga and T.H. Choua, *Colloids and Surfaces A: Physicochem. Eng. Aspects*, 2013, **436**, 1083–1091.
22. J. Perlo, C.J. Meledandri, E. Anardo, D. F. Brougham, *J. Phys. Chem. B*, 2011, **115** (13), 3444–3451.
23. M. F. Roberts, A. G. Redfield, and U. Mohanty, *Biophys. J.*, 2009, **97** (1), 132–141.
24. R. Machán and M. Hof, *Biochimica et Biophysica Acta*, 2010, **1798**, 1377–1391.
25. C. Roobala and Jaydeep K. Basu, *Soft Matter*, 2017, **13**, 4598–4606.

26. W. L. C. Vaz, R. M. Clegg, and D. Hallmann, *Biochemistry*, 1985, **24**, 781-786.
27. M. Bée, *Quasielastic Neutron Scattering* **1988**, Adam Hilger, Bristol.
28. S. Busch, C. Smuda, L. Pardo and T. Unruh, *J. Am. Chem. Soc.*, 2010, **132**, 3232-3233.
29. V. K. Sharma, E. Mamontov, D. B. Anunciado, H. O'Neill and V. Urban, *J. Phys. Chem. B*, 2015, **119**, 4460-4470.
30. V. K. Sharma, E. Mamontov, D. B. Anunciado, H. O'Neill and V.S. Urban, *Soft Matter* 2015, **11**, 6755-6767.
31. V. K. Sharma, E. Mamontov, M. Tyagi, S. Qian, D. K. Rai and V. S. Urban, *J. Phys. Chem. Lett.*, 2016, **7**, 2394-2401.
32. D. K. Rai, V. K. Sharma, D. Anunciado, H. O'Neill, E. Mamontov, V. Urban, W.T. Heller, S Qian, *Scientific Reports* 2016, **6**, 30983.
33. L. Toppozini, C. L. Armstrong, M. A. Barrett, S. Zheng, L. Luo, H. Nanda, V. G. Sakai and M. C. Rheinstädter, *Soft Matter*, 2012, **8**, 11839-11849.
34. V. K. Sharma, E. Mamontov, M. Tyagi and V. S. Urban, *J. Phys. Chem. B*, 2016, **120**, 154-163.
35. V. K. Sharma, E. Mamontov, M. Ohl and M. Tyagi *Phys. Chem. Chem. Phys.*, 2017, **19**, 2514-24.
36. M. Trapp, T. Gutberlet, F. Juranyi, T. Unruh, B. Deme, M. Tehei and J. Peters, *J. Chem. Phys.* 2010, **133 (16)**, 164505-164505.
37. V. K. Sharma, D. G. Hayes, V. S. Urban, H. M. O'Neill, M. Tyagi and E. Mamontov, *Soft Matter*, 2017, **13**, 4871.
38. V. K. Sharma, S. Mitra, G. Verma, P. A. Hassan, V. Garcia Sakai and R. Mukhopadhyay, *J. Phys. Chem. B*, 2010, **114**, 17049-17056.
39. V. K. Sharma, S. Mitra, V. Garcia Sakai, P. A. Hassan, J. Peter Embs and R. Mukhopadhyay, *Soft Matter*, 2012, **8**, 7151-7160.
40. V. K. Sharma, H. Srinivasan, S. Mitra, V. Garcia-Sakai, and R. Mukhopadhyay, *J. Phys. Chem. B*, 2017, **121**, 5562-5572.
41. V. K. Sharma, S. Mitra, M. Johnson and R. Mukhopadhyay, *J. Phys. Chem. B*, 2013, **117**, 6250-6255.
42. K. Shibata, N. Takahashi, Y. Kawakita, M. Matsuura, T. Yamada, T. Tominaga, W. Kambara, M. Kobayashi, Y. Inamura, T. Nakatani, et al., *JPS Conf. Proc.*, 2014, **8**, 036022.

43. R. P. Giri, M. K. Mukhopadhyay, M. Mitra, A Chakrabarti, M. K. Sanyal, S. K. Ghosh, S. Bera, L. B. Lurio, Y. Ma, and S. K. Sinha, *Europhys. Lett.*, 2017, **118**, 58002
44. T. A. Heimburg, *Biophys. J.*, 2000, **78**, 1154–1165
45. R.T. Azuah, L.R. Kneller, Y. Qiu, P.L.W. Tregenna-Piggott, C.M. Brown, J.R.D. Copley, and R.M. Dimeo, *J. Res. Natl. Inst. Stan. Technol.*, **2009**, *114*, 341.
46. M. J. Saxton, *Curr. Top. Membr.*, 1999, **48**, 229–282.
47. P. F. F Almeida, W. L. C. Vaz, T. E. Thompson, *Biochemistry*, 1992, **31**, 6739–6747.
48. F. Volino and A. J. Dianoux, *Mol. Phys*, 1980, **41**, 271-279.

